

Microscopic Selection of Fluid Fingering Patterns

David A. Kessler*

Dept. of Physics, Bar-Ilan University, Ramat-Gan, Israel

Herbert Levine†

Dept. of Physics, University of California, San Diego, 9500 Gilman Drive, La Jolla, CA 92093-0319

(Dated: February 8, 2008)

We study the issue of the selection of viscous fingering patterns in the limit of small surface tension. Through detailed simulations of anisotropic fingering, we demonstrate conclusively that no selection independent of the small-scale cutoff (macroscopic selection) occurs in this system. Rather, the small-scale cutoff completely controls the pattern, even on short time scales, in accord with the theory of microscopic solvability. We demonstrate that ordered patterns are dynamically selected only for not too small surface tensions. For extremely small surface tensions, the system exhibits chaotic behavior and no regular pattern is realized.

PACS numbers: 47.15.Hg, 47.20.Hw, 68.10.-m, 68.70.+w

There has been a continuing debate regarding the issue of the selection of viscous fingering patterns in the limit of small surface tension. On the one hand, the role of surface tension in determining a unique stable steady-state finger through the microscopic solvability mechanism [1, 2] has led to the belief that the details of the small-scale restabilization control the observed patterns, notably including the selection of a single finger filling half the channel from a family of such fingers found initially by Saffman and Taylor [3]. Other researchers [4, 5, 6] have proposed various selection criteria which do not invoke the presence of a microscopic cut-off, and therefore may be entitled macroscopic selection. Here, we perform detailed simulations of anisotropic fingering and demonstrate conclusively that no macroscopic selection occurs in this system.

Viscous fingering, wherein a low viscosity fluid invades a more viscous one in a Hele-Shaw channel geometry, (see Fig. 1), first described by Saffman and Taylor [3], is one of the classic pattern forming systems and serves as the basis for much of our intuition regarding pattern formation. Saffman and Taylor showed both theoretically and experimentally that this system exhibits a pattern-forming instability, an instability that is restabilized at short length scales by the action of the surface tension between the two immiscible fluids. Detailed studies [1, 7, 8, 9] of steady-state propagating finger solutions in this system have revealed the following: At zero surface tension there exists a continuous family of solutions, with continuously varying velocity and asymmetry. At any finite value of the surface tension, γ , this family is reduced to a discrete infinity of symmetric solutions, of which only the most narrow (and fastest) is linearly stable. As γ is reduced toward zero, all these solutions approach a width that is a fraction $\lambda = 1/2$ of the channel width. The physical interpretation of these results has proven very controversial. The claim has been made that it is physically unreasonable for extremely small surface tension to “select” the $\lambda = 1/2$ finger in times of order 1, from a continuum of fingers whose curvatures are never large and should therefore all be essentially unaffected by the surface tension. It

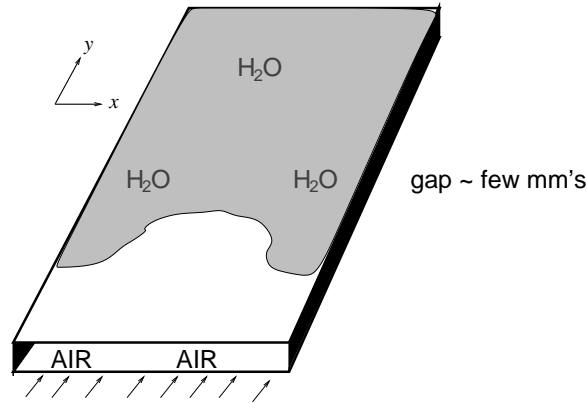


FIG. 1: Schematic of the viscous fingering setup. A Hele-Shaw cell is filled with a viscous fluid (here water) and a less viscous fluid (here air) is injected uniformly from one end. The result is a finger propagating down the channel (in the direction of increasing y).

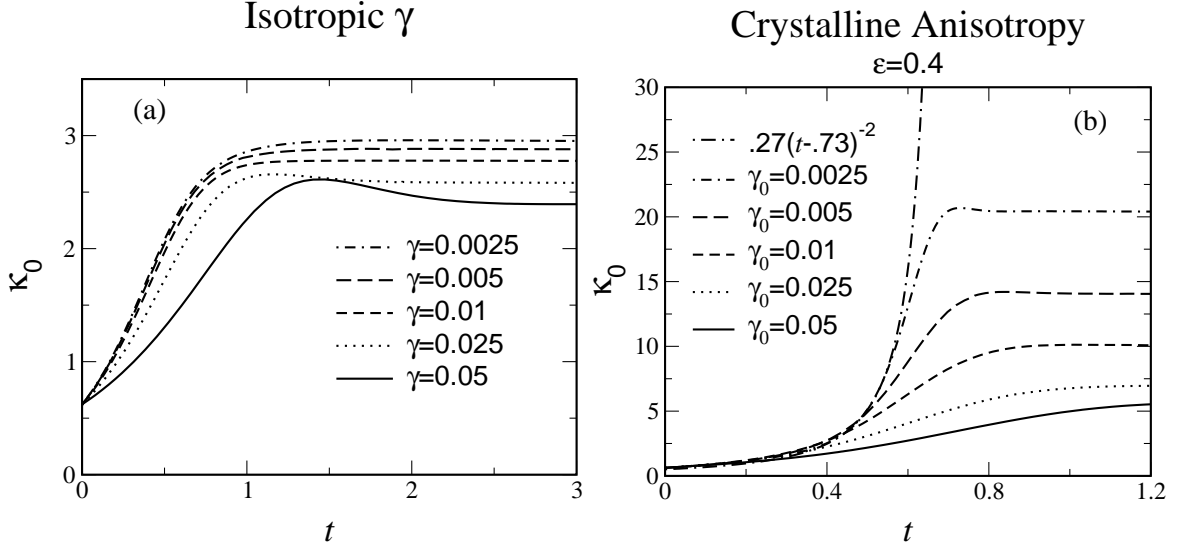


FIG. 2: (a) Tip curvature κ_0 vs. t for various values of isotropic surface tension, γ , starting from identical initial conditions of a small symmetric perturbation. (b) Same for case of crystalline anisotropic surface tension with $\epsilon = 0.4$. The number of points on the interface, N , was taken between 200 and 800, depending on γ . The local relative error of the Gear's method integrator was fixed at 10^{-6} .

is been argued that some other, macroscopic, criteria, must then be responsible for the dynamically chosen $\lambda = 1/2$ finger. We will demonstrate in the following that these claims are incorrect, and indeed the microscopic regularization provided by the surface tension is dynamically relevant and indeed controls the pattern selection.

Part of the difficulty in unraveling the puzzle of selection is that both proposed selection paradigms lead to the same $\lambda = 1/2$ finger at small surface tension. It is thus useful to consider a situation where the two mechanisms would lead to different results. Such is the case of viscous fingering with a crystalline anisotropy of the surface tension. Here the boundary condition for the pressure on the interface, p_{int} , instead of the standard $p_{int} = -\gamma\kappa$, (for surface tension γ and $\kappa = -y''(x)/(1 + y'(x)^2)^{3/2}$ being the curvature of the interface), takes the form

$$p_{int} = -\gamma_0(1 - \epsilon \cos 4\theta)\kappa \quad (\text{Crystalline anisotropy}) \quad (1)$$

where θ is the angle made by the interface normal to the overall flow direction, \hat{y} . This form is familiar from studies of

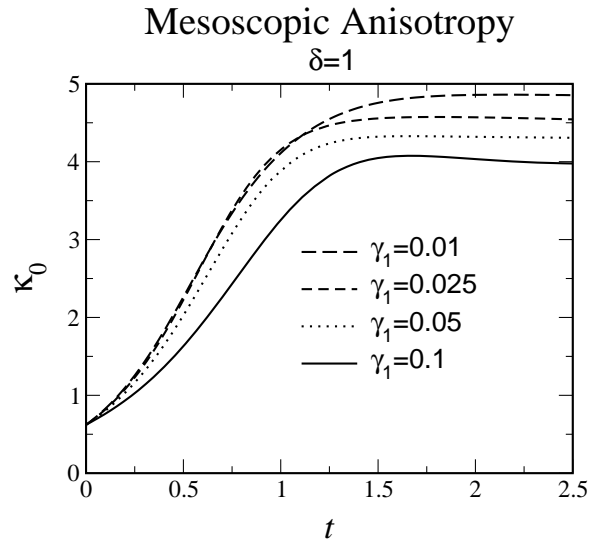


FIG. 3: Simulation of $\kappa_0(t)$ using cutoff (B), with $\delta = 1$ and varying γ_1 . The method and initial condition are the same as in Fig. 2.

dendritic crystal growth [2, 10] and has already been used to model experiments with artificially imposed anisotropy [11, 12, 13, 14]. Study of the steady-state finger with crystalline anisotropy has revealed [10, 15] that for any positive ϵ , the unique stable finger is narrowed, with a width of order $\gamma_0^{1/2}$ for small γ_0 (a scaling identical to that of dendritic solidification of a solid with crystalline anisotropy). Investigation of the dynamics of such an anisotropic system should thus reveal the competition between a macroscopic selection mechanism, if it existed, with its favoring of the $\lambda = 1/2$ finger, and the surface tension which now favors a very narrow finger. We do this by solving the initial value problem (for an inviscid pushing fluid) to see when and how the steady-state is achieved. In Fig. 2, we present the results of this simulation, graphing the tip curvature, κ_0 , as a function of time for varying γ . The simulations were performed via the boundary integral technique described in Refs. [11, 12]. The interface is parametrized by $\theta(\alpha)$ where $0 \leq \alpha \leq 1$ is the relative arclength, and reflection symmetry of the finger is assumed. The initial interface was chosen slightly perturbed,

$$\theta(\alpha) = 0.2 \sin(\pi\alpha) . \quad (2)$$

In Fig. 2a, the results for isotropic surface tension are presented. We see that κ_0 quickly rises, saturating at a γ dependent value slightly below the value of π which characterizes the $\lambda = 1/2$ Saffman-Taylor finger. (The Saffman-Taylor finger is given by the curve $y(x) = \frac{2(1-\lambda)}{\pi} \ln \cos(\frac{\pi x}{2\lambda})$). The selection occurs on a time scale essentially independent of γ , leading apparent credence to the idea that the selection mechanism is independent of γ . In Fig. 2b, however, we present the results of the same simulation, now performed with crystalline anisotropy, with the anisotropy parameter fixed at $\epsilon = 0.4$. If the selection was driven by macroscopic effects, the pattern should be insensitive to the precise form of the surface energy for short and intermediate times. For such times, the data should, for short and intermediate times, recapitulate that of Fig. 2a. Only at long times, times that diverge as $\gamma_0 \rightarrow 0$, should the narrow finger of the steady-state theory emerge. This is not at all what occurs. Instead, the selection of a narrow finger with large tip curvature actually is faster than for the isotropic case, with the selection time actually decreasing with decreasing γ . This is also consistent with the experimental finding that imposing anisotropy creates dendritic structures on a fast time scale [13].

The generalization for dynamics of the microscopic solvability theory of the steady state that emerges from these simulations (see also Ref. [16]) is that as the regularization embodied in the pressure boundary condition is removed, the system tracks some particular time-dependent zero-surface tension solution [16]; but, one cannot determine which of those solutions is selected by any macroscopic construction. The existence of multiple trajectories emanating from arbitrarily close initial conditions is a consequence of the Hadamard ill-posed nature of the $\gamma = 0$ problem [17]. Fig. 2b shows that the selected dynamics with crystalline anisotropy is well-approximated by the curve $\kappa_0(t) \simeq C(t^* - t)^{-2}$ until such time as it saturates to $\kappa_0(\infty) \sim \gamma_0^{-1/2}$. This behavior is exactly what is expected based on the above principle. As pointed out by Howison [18] and also by Shraiman and Bensimon [19], the zero-surface tension dynamics generically exhibits finite-time singularities leading to cusped interfaces with infinite curvature. It was shown that these cusps can be characterized as places where the conformal map $z \equiv x + iy = F(\xi)$ which maps the exterior of the unit circle to the actual flow domain becomes singular via having a zero of $\frac{dF}{d\xi}$ reach the unit circle from its interior. Assume this happens at time t^* and, without loss of generality, at zero phase; we will also assume for simplicity that there is no tangential component of the singularity velocity, since we are dealing with symmetric initial conditions. (It is easy to check that this restriction changes nothing.) Near this time, we have [18, 19]

$$F(e^{i\theta}) \simeq K \left(e^{i\theta} - \frac{t}{t^*} \right)^2 . \quad (3)$$

This leads to the parametric curves

$$\begin{aligned} x(\theta) &\simeq -K(2 - t/t^*)\theta^2 + \text{constant} \\ y(\theta) &\simeq K(\theta(1 - t/t^*) - \theta^3) \end{aligned} \quad (4)$$

Hence, the curve approaches the cusp structure $|x| \simeq |y|^{2/3}$ via the blow-up $\kappa_0 \simeq x''(y) \simeq C/(t^* - t)^2$. Thus, this form of anisotropic surface tension has selected the zero-surface tension solution with a finite-time singularity, rather than the $\lambda = 1/2$ finger. Moreover it has done so on a time scale independent of γ . Clearly which pattern is dynamically selected (even on short time scales) is controlled by the surface tension, despite its smallness.

We have seen that we can, by picking a suitable surface tension, cause either the $\lambda = 1/2$ or the near-cusp solution (with tip curvature proportional to $\gamma^{-1/2}$, although $\gamma\kappa$ at the tip is still small) to be selected. In fact, by a suitable form of surface tension anisotropy, for example,

$$p_{int} = \gamma_1 \frac{y''(x)}{(1 + \delta + y'(x)^2)^{\frac{3}{2}}} \quad (\text{Mesoscopic anisotropy}) \quad (5)$$

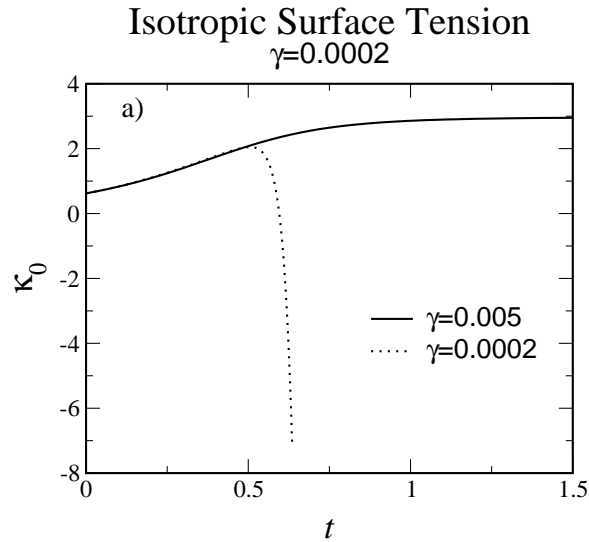


FIG. 4: Simulation of $\kappa_0(t)$ for isotropic surface tension $\gamma = 0.0002$ and the same initial condition as in Fig. 2. Here $N = 1000$ and the relative error 10^{-9} .

we can select any $\lambda (< 1/2)$ we choose. In Fig. 3, we present our results for this mesoscopic anisotropy, showing that now the system chooses, in finite time, a finger with tip curvature which approaches a finite value significantly greater than π . Again, there is no sign of a macroscopically selected finger of width λ equal to $1/2$. To understand our result, we note that solvability theory [10] predicts that the width is determined by matching the complex-plane singularity in the modified curvature that occurs when $y'(x) = i\sqrt{1+\delta}$ with a zero of the function $g(y') \equiv y''(y'(x))$. For the finger,

$$g(y') = \frac{\pi(1-\lambda)}{2\lambda^2} \left(1 + \left(\frac{\lambda y'}{1-\lambda} \right)^2 \right) \quad (6)$$

vanishes at $y' = i(1-\lambda)/\lambda$, giving the selected values

$$\begin{aligned} \lambda &= \frac{1}{1 + \sqrt{1+\delta}} , \\ \kappa_0 &= \frac{\pi}{2} \sqrt{1+\delta} (1 + \sqrt{1+\delta}) . \end{aligned} \quad (7)$$

This result is in good agreement with our simulations and rules out any macroscopic selection. Rather, the detailed form of the microscopic re-stabilization indeed determines the selected pattern.

However, by no means is this the whole story. We saw in Fig. 2a how reducing γ for the usual isotropic surface tension appeared to yield a limit curve which asymptotes to the selected $\kappa_0 = \pi$ corresponding to $\lambda = 1/2$. Let us examine what happens for an even smaller γ with exactly the same initial conditions. We see in Fig. 4 that κ starts out as before, but then turns down, going negative, due to a splitting of the tip [1, 20, 21]. How are we to understand this, given the demonstration [22, 23, 24, 25] of the linear stability of the selected finger for all surface tension? The explanation is that the size of the basin of attraction of the $\lambda = 1/2$ steady state finger is γ dependent, becoming smaller (exponentially quickly) as $\gamma \rightarrow 0$ [22, 23].

Thus, the complaint that extremely small surface tension is incapable of selecting the finger width is perfectly correct – at such small surface tensions, indeed, no steady-state finger is selected. Rather, it is likely the system is chaotic, generating a random succession of tip-splittings similar to that seen in the Diffusion-Limited-Aggregation model [26] of Laplacian growth, where noise is added explicitly. We can see this by examining the divergence of two nearby trajectories, as shown in Fig. 5. Two runs with very slightly different initial conditions were performed, the first as in Eq. 2 and the second with the size of the initial perturbation 0.001% larger. We find that initially the difference in $\kappa_0(t)$ slowly increases in a linear fashion, but eventually rises exponentially, increasing by over two orders of magnitude. Presumably, as γ is reduced to zero, the maximal Lyapunov exponent diverges, giving rise to the Hadamard ill-posedness of the zero γ problem. Selection of the $\lambda \approx 1/2$ finger is thus seen as a kind of intermediate

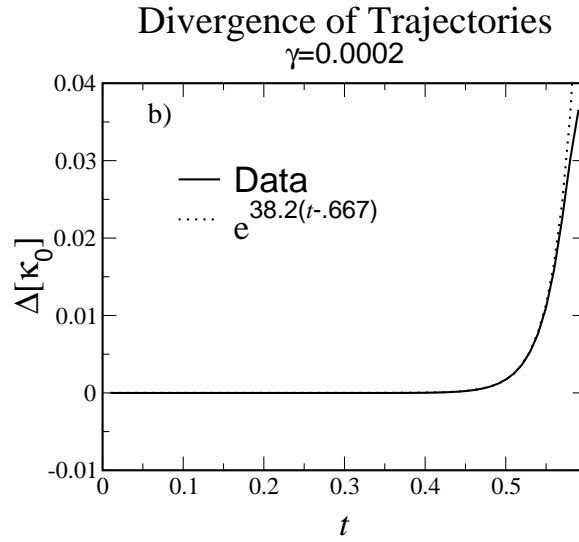


FIG. 5: Difference of $\kappa_0(t)$ for two runs with isotropic surface tension $\gamma = 0.0002$ and slightly different initial conditions. Here, $N = 200$ and the relative error 10^{-8} .

asymptotics, realized for small but not too small γ . Those searching for a macroscopic selection principle to account for selection of $\lambda = 1/2$ at extremely small surface tension are then searching for the solution to a nonexistent dilemma.

DAK wishes to thank Prof. Lee Segel for a careful reading of the manuscript. The work of DAK is supported by the Israel Science Foundation. The work of HL is supported by the National Science Foundation grant DMR-98-5735.

* Electronic address: kessler@dave.ph.biu.ac.il

† Electronic address: hlevine@ucsd.edu

- [1] D. A. Kessler, J. Koplik and H. Levine, *Adv. Phys.* **37**, 255 (1988).
- [2] J. Langer, *Science*, **243**, 1150 (1989).
- [3] P. G. Saffman and G. I. Taylor, *Proc. Roy. Soc. A* **245**, 312 (1958).
- [4] M. J. Feigenbaum, I. Procaccia and B. Davidovich, preprint, chaos-dyn/9908007.
- [5] A. Aldushin and B. J. Matkowsky, *Phys. Fluids* **11**, 1287 (1999).
- [6] M. Mineev-Weinstein, *Phys. Rev. Lett* **80** 2113 (1998).
- [7] G. M. Homsy, *Ann. Rev. Fluid Mech.*, **19**, 271 (1987).
- [8] D. Bensimon, et. al., *Rev. Mod. Phys* **58**, 977 (1986).
- [9] S. Tanveer, *J. Fluid Mech.* **409**, 273 (2000).
- [10] D. A. Kessler, J. Koplik and H. Levine, *Phys. Rev. A* **34**, 4980 (1986).
- [11] D. A. Kessler, J. Koplik and H. Levine, *Phys. Rev. A* **30**, 3161 (1984).
- [12] G. Li, D. Kessler, and L. Sander, *Phys. Rev. A* **34**, 3535 (1986).
- [13] E. Ben-Jacob, et al *Phys. Rev. Lett.* **55**, 1315 (1985).
- [14] K. V. McCloud and J. V. Maher, *Phys. Rep.* **260**, 139 (1995).
- [15] A. T. Dorsey and O. Martin, *Phys. Rev. A* **35**, 3989 (1987).
- [16] A. Sarkissian and H. Levine, *Phys. Rev. Lett* **81**, 4528 (1998).
- [17] A. S. Fokas and S. Tanveer, *Math. Proc. Cambridge Phil. Soc.* **124**, 169 (1998).
- [18] S. D. Howison, *Siam J. Appl. Math.* **46**, 20 (1986).
- [19] B. Shraiman and D. Bensimon, *Phys. Rev. A* **30**, 2840 (1984).
- [20] A. R. Kopf-Sill and G. M. Homsy, *Phys. Fluids* **31**, 242 (1988).
- [21] M. W. DiFrancesco and J. V. Maher, *Phys. Rev. A* **39**, 4709 (1989).
- [22] D. A. Kessler and H. Levine, *Phys. Rev. A* **33**, 2621 (1986).
- [23] D. Bensimon, *Phys. Rev. A* **33**, 1302 (1986).
- [24] D. A. Kessler and H. Levine, *Phys. Fluids* **30**, 1246 (1987).
- [25] S. Tanveer, *Phys. Fluids* **30**, 2318 (1987).
- [26] T. A. Witten and L. M. Sander, *Phys. Rev. B* **27**, 5686 (1983).